
IMPROVING PARAMETRIC NEURAL NETWORKS FOR HIGH-ENERGY PHYSICS (AND BEYOND)

IN PREPARATION

✉ Luca Anzalone, ✉ Tommaso Diotallevi, ✉ Daniele Bonacorsi

Department of Physics and Astronomy (DIFA)

University of Bologna

Bologna, BO 40127

{luca.anzalone2, tommaso.diotallevi, daniele.bonacorsi}@unibo.it

February 3, 2022

ABSTRACT

Signal-background classification is a central problem in High-Energy Physics (HEP), that plays a major role for the discovery of new fundamental particles. A recent method – the Parametric Neural Network (pNN) [4] – leverages multiple signal mass hypotheses as an additional input feature to effectively replace a whole set of individual classifier, each providing (in principle) the best response for a single mass hypothesis. In this work we aim at deepening the understanding of pNNs in light of real-world usage. We discovered several peculiarities of parametric networks, providing intuition, metrics, and guidelines to them. We further propose an alternative parametrization scheme, resulting in a new parametrized neural network architecture: the AffinePNN; along with many other generally applicable improvements. Finally, we extensively evaluate our models on the HEPMASS dataset [3], along its *imbalanced* version (called HEPMASS-IMB) we provide here for the first time to further validate our approach. Provided results are in terms of the impact of the proposed design decisions, classification performance, and interpolation capability as well.

Keywords Parametric Neural Networks · Deep Learning · High-Energy Physics

1 Introduction

When searching for new particles, physicists are really interested in rare events (yield by the collision of known particles) that possibly follow their theoretical assumptions. These rare events – the so-called *signal* – must be separated out from the *background*, i.e. anything else originated from already known processes. Being able to effectively separate background events from the *signal* is a central problem in HEP, that can help the discovery of new fundamental particles with further analysis [7]. Unfortunately, the signal is not known and so classification systems, like (boosted) decision trees (DTs) [15, 7] and neural networks (NNs) [16, 5], are trained on synthetic data obtained through expensive Monte-Carlo simulations, that try to mimic data coming from real-world collisions of particles. Moreover, is not possible to know in advance whether the kind of signal we are looking for *really exists* on the new inference data.

Before the introduction of parametrized neural networks (pNNs) [4] (described in section 2.1), the canonical approach for signal-background classification consisted of training a set of *individual and independent classifiers* [5], each of them trained on a specific signal mass hypothesis $m_i \in \mathcal{M}$ (thus, on a subset of the available data, somehow). The benefit of individual classifiers is that each of them should maximize the separation of the two classes for a single mass hypothesis. The major drawback is that researchers have to design, train, tune, evaluate, and maintain $|\mathcal{M}|$ of such classifiers, one for each mass¹ ($m_i \in \mathcal{M}$), often with different hyperparameters, whose

¹Here the term *mass* refers to a theoretical parameter, which we also call m_A , that is the additional input of the parametric network: also called *mass feature* by Baldi et al [4]. The theoretical parameter (m_A) corresponds to the mass hypotheses (\mathcal{M}) at which the signal was generated, and not the reconstructed mass of the considered decay.

amount can easily be in the order of tens or twenties: this can become easily unfeasible. The other issue is about classification performance. Specifically talking about neural networks, they greatly benefit from the *sharing of weights* and *distributed representation* [16] for improved accuracy, reduced training time, and thus increased data efficiency. Parametric neural networks aim at mitigating those issues by means of an additional input (the signal's generating mass), while also bringing additional benefits for the sake of more effective research.

The overall contributions of our work are summarized as follows:

- We propose a novel and more challenging benchmark dataset called HEPMASS-IMB (section 3.1.1), to overcome the simplicity of HEPMASS [3], trying to emulate real-world scenarios more closely.
- We developed a novel parametrization scheme: the *affine parametric neural network* (section 4.1).
- We describe and empirically study several design decisions for building effective pNNs (section 4). In this regard, we address the issue of how to assign (or distribute) the mass feature for the background events (section 4.2). As well as providing a novel *balanced training* procedure (4.3).
- We attempt a first characterization of the *properties* that parametric networks have (section 5).
- Regarding interpolation (section 5.1), we study it in dept: showing a failure case, and providing guidelines for its assessment.

2 Related Work

2.1 Parametric Neural Networks

A *parametric neural network* (pNN) [4, 19, 11] is a neural network architecture that leverages an additional input (in our case the *mass* of the hypothetical particle) to replace many individual classifiers, and potentially even improve their classification performance. Let be x the input features, m the generating mass of the signal (or the signal mass hypotheses), and θ a set of learnable weights (or parameters); a pNN can be denoted as $f_\theta(x, m)$, i.e. as a learnable function of both the input features x and the *mass feature* m . A canonical neural network, instead, would be denoted as $f_\theta(x)$, depending only on one input: the features.

Indeed the idea of "parametric" is not new, as in other fields of machine learning, like *imitation learning* [9], *multi-task & meta-learning* [14], *unsupervised reinforcement learning* [13], and *deep generative models* [18], is commonly called "conditioning". Here the general idea is to condition the learning (i.e. output) of a neural network on some additional representation z , in order to let the network's output change as z varies. The vector z – called the *task representation* – can take various forms: ranging from a one-hot encoding to a dense embedding, or be a single discrete or continuous variable as well. In our case, the mass feature (i.e. the task representation) is a single scalar m belonging to a finite set $\mathcal{M} = \{m_1, m_2, \dots, m_M\}$ of mass hypotheses about the signal process we're interested in.

This idea, whether called conditioning or parametrization, is promising in HEP since it may enable to replace (potentially many) individual classifiers with a unique classifier trained on all mass hypotheses; thus, leveraging *sharing of weights* for more efficient learning, and *distributed representations* shared among mass hypotheses for improved predictions, which we also found to be beneficial in *low-data regimes*: i.e. when some of the data corresponding to certain masses, is *imbalanced* compared to the most representative masses². The authors also claim that, since the additional input would define a "*smoothly varying learning task*", a pNN would be able to "*smoothly interpolate*" between such learning tasks. Ideally, this means that a pNN would be able to generalize (correctly classify events) beyond the mass hypotheses it was trained on, thanks to the additional mass feature.

In this case, our supervised dataset \mathcal{D} have the form $\{(x, m, y)_i\}_{i=1}^N$, in which we have input features x (i.e. the variables associated to each event), their mass hypothesis m , and the target class labels y we aim to predict. For each signal mass hypothesis, $m_i \in \mathcal{M}$, we can *slice* our dataset such that only the features and targets corresponding to mass m_i are retained, i.e. $\mathcal{D}_{m_i} = \{(x, y)_j : m_j = m_i, \forall j = 1, \dots, N\}$, where N is the total number of events³. In this way, we obtain $|\mathcal{M}|$ datasets for which each of them can be used to train an individual classifier (but also to evaluate our pNN at single mass points). The pNN can replace all of them, and if trained on a subset of the mass hypotheses, $\bar{\mathcal{M}} \subset \mathcal{M}$, it is, in principle, able to automatically account for the missing masses ($\tilde{m}_j \in \mathcal{M} \setminus \bar{\mathcal{M}}$) thanks to the interpolation capability (discussed in section 5.1), which should work on novel intermediate mass points as well.

²This is often the case in practice, since when doing MC simulations to produce the data, some kind of events (for certain masses) are more frequently generated (thus being less rare) than others, naturally resulting in an *imbalanced dataset*, that is imbalanced not with respect the class labels (since the background class is independently produced) but with respect the *mass labels*.

³From a ML jargon perspective we can equivalently refer to events as (ex)amples or datapoints, of some dataset.

2.2 Conditioning Mechanisms

The authors of the original pNN [4] utilize a simple conditioning mechanism: they simply *concatenate* the features with the mass (or task representation, in general) obtaining a new set of features, $\tilde{x} = [x, m]$, going back to a standard feed-forward neural network formulation, i.e. $f_\theta(\tilde{x})$, that learns from an *extended* set of features \tilde{x} . Indeed, many arbitrarily-complex conditioning mechanisms exist, two of them (figure 1) are yet simple but powerful [12]:

- **Concatenation-based conditioning:** the task or conditioning representation m (our mass) is first concatenated along the last dimension (axis) of the input features x , and then the result is passed through a linear layer. Notice that in the original pNN, the linear layer after concatenation is missing.
- **Conditional scaling:** a linear layer first maps the conditioning representation m to a scaling vector s , to which follows an element-wise multiplication (Hadamard product) with the input features x , i.e. $x \odot s$.

These two conditioning mechanisms are widely applicable, although it's not yet clear in which case one mechanism is preferable to the other(s). Anyway, these two mechanisms can be both combined into a third one⁴: a *conditional affine transformation* [12], which motivates our new parametric architecture (refer to section 4.1).

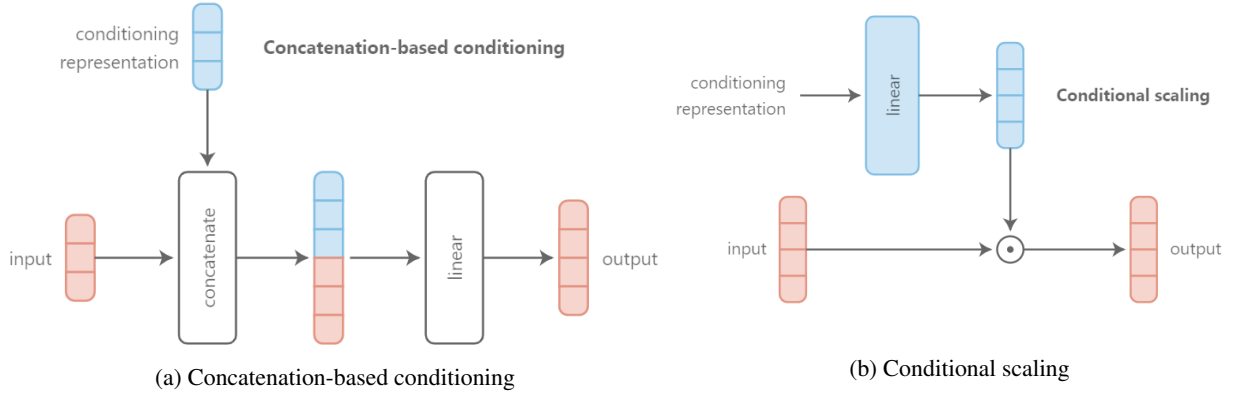


Figure 1: Two popular conditioning mechanisms, that tuned out to be complementary. Figure adapted from [12].

3 Datasets

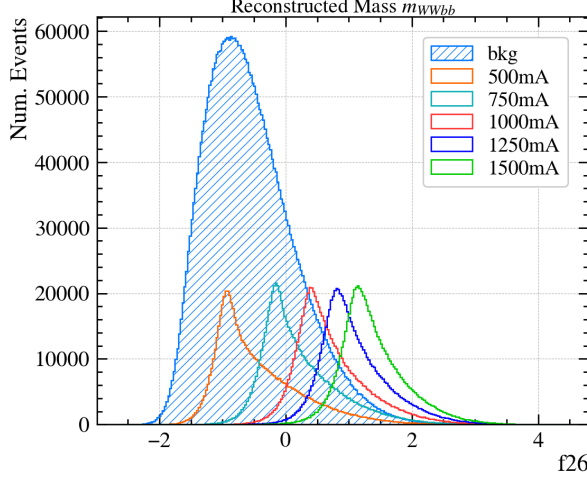
3.1 HEPMASS

The HEPMASS dataset [3, 4] was utilized by the pNN's authors to demonstrate their novel idea. The dataset contains 7M training samples, and 3.5M test samples. There are a total of 27 features (without considering the 28-th *mass feature*) already normalized to have approximately zero-mean and unitary variance. Each datapoint x can belong to one of five mass hypotheses (GeV), $\mathcal{M} = \{500, 750, 1000, 1250, 1500\}$, and is labeled with either 1 (signal) or 0 (background): for samples of the background class, the values of the mass feature were randomly sampled from \mathcal{M} . Moreover, the two classes are perfectly balanced, and also each \mathcal{D}_{m_i} is *balanced*: containing the same amount of events for each $m_i \in \mathcal{M}$. As discussed in the previous section, when training pNNs we want to pay attention to the balance of classes as well as the balancing of each mA: this dataset avoids such issue. For further details about the dataset, refer to [4].

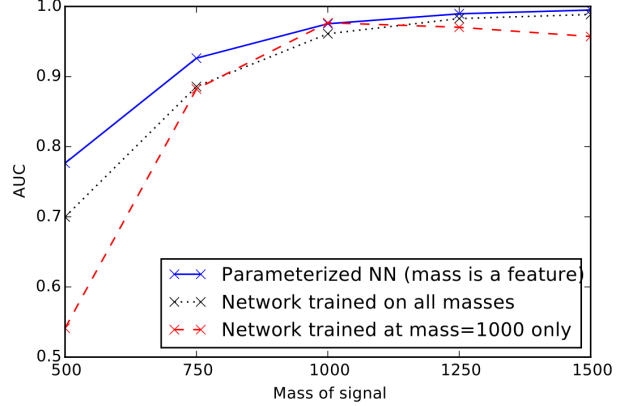
By studying the distribution of each feature we can deduce three major things:

1. The background is unique and covers the signal, although partially (figure 2a).
2. By only considering some features (figure 3) a classifier (even simple) can easily tell which event belongs to the signal-class or not.
3. Conversely, the signal's events at 500mA are the most difficult to separate out from the background since the features distribution is mostly completely overlapped with the background's one. This explains why the AUC is considerably lower for 500mA, while being almost perfect for 1500mA.

⁴An affine transformation, i.e. $y = Ax + b$, does not involve concatenation directly: turns out that concatenation-based conditioning is equivalent to *conditional biasing*, in which the task representation is first mapped to a bias vector that is then added to the input, element-wise, effectively replacing a concatenation operation. Further details in [12].

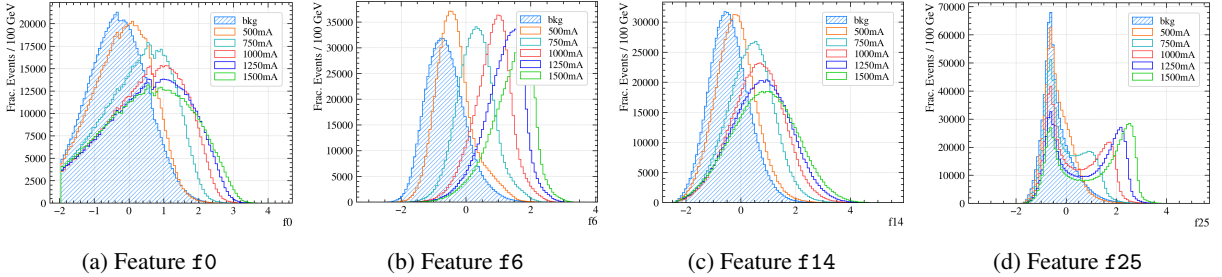


(a) Distribution of feature f26: the whole background class is represented in blue, whereas each signal m_A with a different color.



(b) Per-mass AUC of the ROC: figure from [4].

Figure 2: According to figure (a) and [4], the feature f26 should correspond to the *reconstructed mass*, m_{WWbb} , of the simulated particle ($X \rightarrow t\bar{t}$) depicted in HEPMASS. If so, we observe that the background spans the entire mass range, mostly overlapping the signal at 500 and 750mA. This fact also motivates why the authors' results (and our own) exhibit a neat loss in AUC below 750 GeV, especially at 500mA.



(a) Feature f0

(b) Feature f6

(c) Feature f14

(d) Feature f25

Figure 3: Some features in which we can clearly observe how easily the distribution of each signal mA drifts away from the background. In particular, the distribution of 500mA almost completely overlaps with the background, each time; telling us that these events are the most difficult to classify (as shown in figure 2b).

3.1.1 HEPMASS-IMB

Since the HEPMASS dataset is rather simple, leaving almost no room for improvement, we decided to *imbalace* the dataset by hand in order to being able to demonstrate novel methods for improving pNNs: we call this new dataset HEPMASS-IMB. In particular the dataset is *doubly-imbalanced*: there is a *class-imbalance* w.r.t. the class label, and a *mass-imbalance* w.r.t. the theoretical parameter (m_A), as well. A comparison between the two dataset is depicted in table 1.

The way we imbalance the dataset is as follows: indeed, we only imbalance the train-set of HEPMASS, leaving its test-set as it was provided by the authors [3]. We first take all the background events (without any change), and so sub-sample (without replacement) only the signal, differently at each m_A . In particular we keep: 350k (for 500mA), 140k (for 750mA), 35k (for 1000mA), 7k (for 1250mA), and lastly 2k events for 1500mA; for a total of almost 534k signal events. In such way we are able to simulate a double imbalance of both class-labels and signal mass hypotheses (figure 5), that resembles more the imbalance found in real-world dataset of Monte-Carlo simulated particle decays.

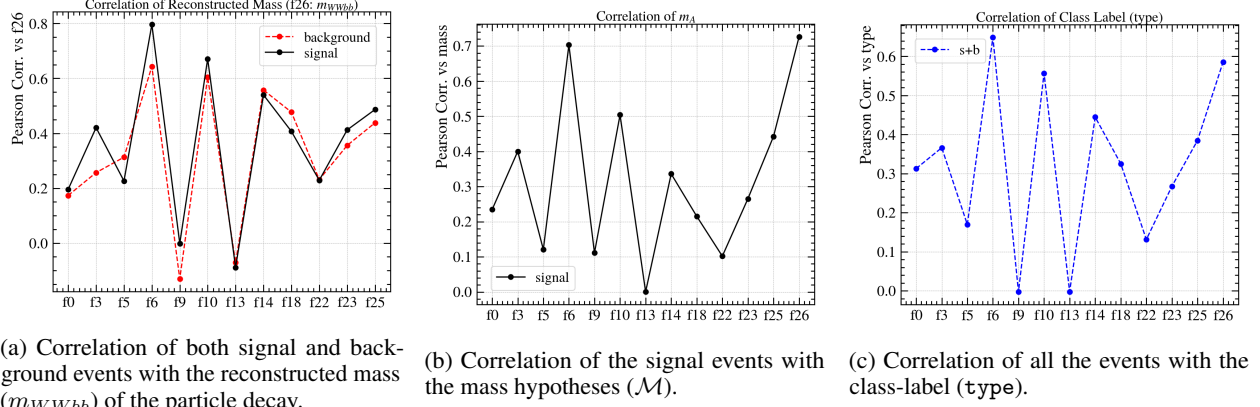
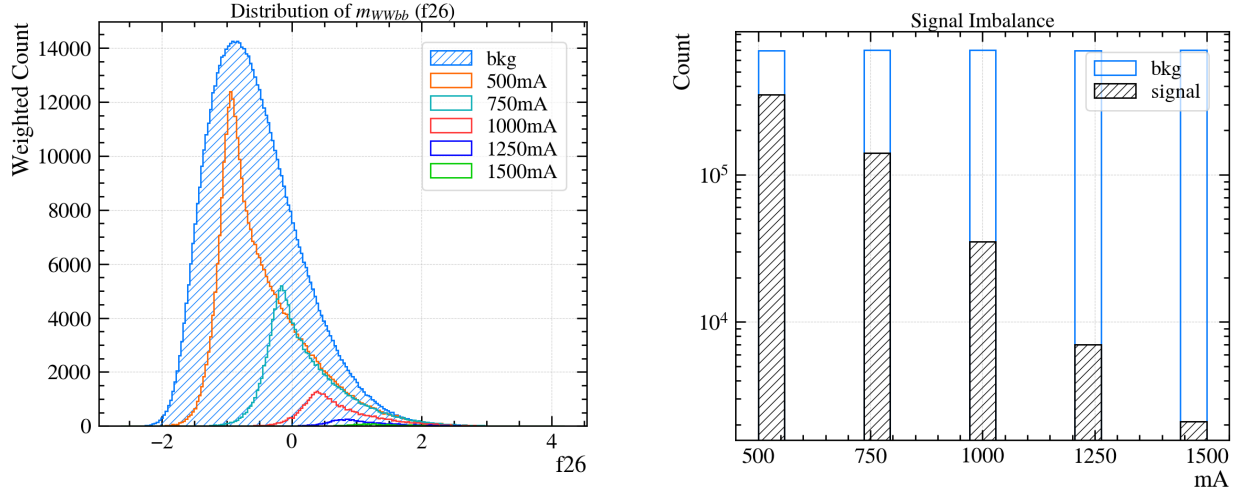


Figure 4: Pearson correlations of the training variables of HEPMASS (train-set).



(a) Resulting distribution of the reconstructed mass after having imbalanced HEPMASS. Compared to figure 2a, we can see how less the signal is: the background has been weighted by 1/5, for visualization purpose.

(b) Imbalance of all the \mathcal{M} signal mass hypotheses: log-scale. We can see that the imbalance ratio grows with the m_A , for a maximum difference of few orders of magnitude.

Figure 5: Overall class and mass imbalance of HEPMASS-IMB.

4 Design Choices

Having the extra *mass feature* as input gives us an additional degree of freedom for the design of classifiers. In this section we study different design decisions about *network architecture*, *background distribution*, and *training procedure*.

4.1 The Affine Architecture

Baldi et al [4] utilized a regular *feed-forward* design for their parametric network, which we will refer to (vanilla) *pNN*, by just concatenating the mass feature m with the input features x right after the input layer. Here we propose a novel conditioning (or parametrization) scheme to better exploit m , that is based on two simple conditioning mechanisms (figure 1), namely: *conditional scaling*, and *conditional biasing* (equivalent to concatenation-based conditioning).

We propose an *Affine Parametric Neural Network* (AffinePNN) architecture, that relies on multiple *affine-conditioning layers* instead of simply concatenating the mass at the beginning of the network. Such a layer takes both the features x (or previous layer's output) and the mass feature m as input, applying an element-wise affine

Characteristic	Dataset	
	HEPMASS [3]	HEPMASS-IMB (our)
# Samples	7M (+ 3.5M test)	4M (+ 3.5M test)
Class imbalance (%)	None	13 (signal) / 87 (bkg)
Signal imbalance	None	up to $166\times$
Mass hypotheses	5 (equally spaced)	//
# Variables	27	//
Bkg distribution*	identical (fixed)	//
Signal process	$t\bar{t} \rightarrow W^+bW^-\bar{b} \rightarrow qq'bl\nu\bar{b}$	//
Bkg process	$t\bar{t}$	//

Table 1: Datasets comparison. As we can see, our modification of HEPMASS adds more difficulties to be addressed. This allowed us to discover many weaknesses of pNNs. (*) Design decisions about how to best distribute the mass of background events are depicted in section 4.2, going beyond what’s fixed in the datasets.

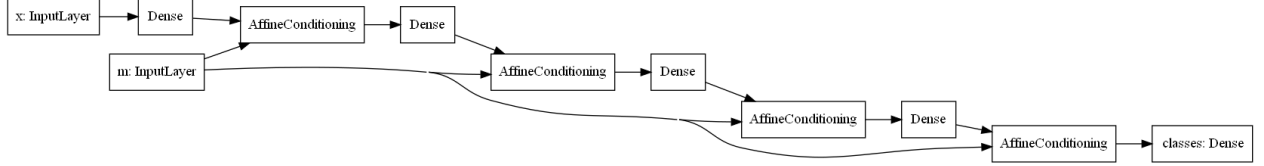


Figure 6: Diagram of the Affine architecture. In this picture the relation between the inputs and the layers can be better understood. At the beginning, the input features x are only fed to the first Dense layer; the mass feature m , instead, are only provided to each AffineConditioning layer. Dropout layer are omitted for clarity.

transformation (scaling and bias addition) on x , such that the output z is a function of m :

$$z = x \odot s_\phi(m) + b_\psi(m)$$

The scaling and biasing coefficients are defined as linear functions over the mass: $s = \phi \cdot m$, and $b = \psi \cdot m$; where ϕ and ψ are learned weights⁵. An AffinePNN interleaves such layers with ReLU-activated⁶ dense layers: see table 2 and figure 6, for an overview of the architecture. In principle, the affine layers can be further generalized by introducing non-linear activation functions (g and h) on the scaling s_ϕ , and bias b_ψ , such that: $z = x \odot g(s_\phi(m)) + h(b_\psi(m))$.

4.2 Background’s m_A Distribution

In our reference work [4] the background’s mass feature is *identically distributed* as the signal’s mass. In other analyses background events receive a mass that is either: (1) *randomly assigned* from the distribution of signal masses (only during training) [10], or (2) *uniform* in the interval of considered mass hypotheses. In general, we can analyze two situations: *identical* and *different* distribution of m_A for background events only.

1. **Identical distribution:** the mass feature for background events is assigned exactly to a value of the finite set $\mathcal{M} = \{m_0, m_1, \dots\}$ of the signal mass hypotheses, selected randomly i.e. $m \sim \mathcal{M}$.
2. **Different distribution:** the theoretical parameter (m_A) is employed to define a probability distribution (e.g. *uniform* in the interval $[\min(\mathcal{M}), \max(\mathcal{M})]$, or *Gaussian* being centered at each $m_i \in \mathcal{M}$) that is *diverse* from (going beyond) the finite set of values that \mathcal{M} encodes. In this work, we only consider a uniform distribution $U(\mathcal{M}_{\min}, \mathcal{M}_{\max})$ for the mass feature, m . Therefore, background events will be assigned a mass feature by sampling randomly from such distribution, i.e. $m \sim U$.

⁵In practice, ϕ and ψ are the weights of two distinct Dense layers.

⁶ $\text{ReLU}(x) = \max(0, x)$, applied element-wise as usual.

Layer	# Units
Input (x and m)	
Dense + ReLU	300
AffineConditioning	300
Dropout	
Dense + ReLU	150
AffineConditioning	150
Dropout	
Dense + ReLU	100
AffineConditioning	100
Dropout	
Dense + ReLU	50
AffineConditioning	50
Dropout	
Dense + Sigmoid	1

Table 2: Affine architecture. Each AffineConditioning(m, z_i) layer takes two inputs: the masses m input to the network, and the output z_i of the previous Dense layer. For better performance Dropout layers are also included, but only after each AffineConditioning layer. Basically, the architecture is made of four *blocks*, in which each block (Dense \rightarrow AffineConditioning \rightarrow Dropout) have, respectively, 300, 150, 100, and 50 hidden units, activated by ReLU non-linearity.

In both cases, we can *fix* the values of the mass feature (only for background) in the dataset (e.g. by sampling m only one time, and writing them to disk), or we can *sample* them during training, repeatedly and differently at each mini-batch. So, we have two degrees of freedom (distribution type, and assignment strategy) that lead us to a total of four unique combinations: (1) *identical fixed*, (2) *identical sampled*, (3) *uniform fixed*, and lastly (4) *uniform sampled*. In our experiments we noticed that, without proper regularization, having a uniform mass feature for the background allowed the network to almost perfectly fit both the training and validation sets: this may be due to the introduction of an artificial correlation between the mass feature and the class label, that was exploited during training. Nevertheless, by regularizing the model enough generalization is still ensured.

We may further discuss an additional assignment strategy where the mass feature m for the background can be also determined by means of *mass intervals* (or bins), based on the underlying *reconstructed mass* of the selected decay products. For example, if we consider (150, 250) to be a specific mass interval centered around 200 GeV, we can assign $m = 200$ as mass feature for each background event x whose reconstructed mass is within the mass interval. In this work, such third assignment strategy have not been taken into account.

4.3 Training Procedure

Beyond the architecture and regularization of the parametric network, also how the parameter m is distributed, we can make some considerations about how to properly train such kind of neural networks in light of what we already known about the structure of our own data. In general, we know that the signal is arranged in $|\mathcal{M}|$ groups (one for each m_A), and that the background is (eventually) composed of different processes. All of this tells us that beyond class labels, our data is naturally divided in *sub-classes*: in terms of the signal generating mass (i.e. the various m_A), and background processes⁷. We can exploit such domain-knowledge to design a training procedure that embeds such *inductive biases*.

In particular, we can further notice that each sub-class may have its own unique *frequency* (in terms of how much data samples fall into each sub-class: see figures 2a and 5b. Such frequencies may bias the (parametric) network towards certain sub-classes, resulting in an overall sub-optimal fitting of the data. We propose to mitigate this simply by

⁷We can think of sub-classes as additional labels in our data.

balancing each sub-class in a way that an equal number of events belongs to each of them. We call such approach *balanced training*, that, without discarding or generating new data, can be easily implemented by balancing each *mini-batch* during training, e.g. by sampling each sub-class in equal proportion. Specifically, we have:

- **No balance:** The usual training procedure, in which the network is trained by experiencing the data as it is. This will be our baseline for comparison.
- **Class-only balance:** Only the class labels are balanced within each mini-batch. Considering two classes, we can balance them in two ways: (1) by associating *sample or class weights* to each event, resulting in a weighted loss function, or (2) by sampling the events for a mini-batch such that half the batch is populated with samples belonging to the positive class (i.e. signal), and the other half with background samples (the negative class). We implement class-balancing by following the second option, in which is as if the class weights were *implicit*.
- **Signal balance:** Since the entire signal is generated at different values of m_A , we can build mini-batches such that there is an equal number of events for each m_A . In practice, we take half the size B of a batch, i.e. $B_s = B/2$, and then split that in even parts such that each $m_i \in \mathcal{M}$ is represented by exactly $B_s/|\mathcal{M}|$ events. Doing so also implies that at each mini-batch all the signal mass hypotheses are always represented: this may not occur, especially if the batch size is small, for no, class and background balancing.
- **Background balance**⁸: Similar to signal balancing, mini-batches are divided in equally-sized parts such that each part contains events that belong to a certain background process. Of course, such balancing strategy is only meaningful if our background comprises more than one process. Also in this case, each mini-batch will contain samples coming from all background processes.
- **Full balance**⁹: A combination of class, signal, and background balance. A batch is divided into two halves (each of size $B/2$) to ensure class balance. Then, one half will be signal balanced, and the other one is balanced according to the background. In this way, the network will always experience mini-batches that comprise all signal hypotheses, as well as all background processes.

4.4 Preprocessing and Regularization

In general, for our models we found out regularization to be beneficial for improved performance, and also (as we will see later) crucial for good interpolation. We utilize two well known regularization techniques: *dropout* [20], and *l2-weight decay*. In particular, we insert a Dropout layer (with a drop probability of 25%) after each hidden Dense layer. Lastly we apply *l2*-regularization on all learnable parameters of the network, but with different coefficients for weights and biases respectively.

Classification performances can be usually further boosted by properly normalizing the data input to the network. Recall that our data have the form (x, m, y) in which: x is a multi-dimensional vector of features, m (the mass feature) corresponds to the masses (or m_A) that makes the network be "parametric", lastly y is a vector of class-labels (either 1 for signal or 0 for background, in our case). Discarding y , we can normalize (or preprocess, in general) both x and m in the same way (as done by [4] by means of *min-max normalization*), or differently. In our case, as HEPMASS is already standardized, we only normalize m by just *dividing* it by 1000.

5 Properties of PNNs

We believe parametric networks to have many interesting properties beyond interpolation. In this section we attempt a first characterization of them, trying to better understand such kind of models.

5.1 Interpolation

The interpolation capability of a parametric neural network is its ability to generalize towards novel mass points that lie between two known mass hypotheses, resulting in effective interpolation of events between them. In this case the generalization capability should be *twofold*: (1) the network is requested to perform well on novel samples belonging to the known masses, and (2) also to correctly classify new events that belong to the missing hypotheses. This means that a network that interpolates well can be trained on less data with a negligible loss in accuracy, allowing us to effectively reduce the number of Monte-Carlo simulations required to generate training events (which are tremendously expensive,

⁸In the specific case of HEPMASS-IMB, due to its single background process the background-only balancing procedure is meaningless.

⁹Our way of implementing both signal-only and fully balanced training (in which half the batch size is reserved for signal, and the other half for background events) makes them to be equivalent for HEPMASS-IMB; not true in general.

especially for some m_A whose signal events are more rare). We want our pNN to perform well even if some hypotheses are missing. So, how to be sure and ensure that our model has acquired such capability?

Factors. We investigated several potential factors, including *per-mass features distribution*, *mass imbalance*, *background distribution*, *network regularization*, *batch size*, and *training procedure*, that may affect the interpolation capability of pNNs. Here we describe the most impactful:

- **Per-mass features distribution:** recall the shift in feature distribution observed as the m_A varies (figure 3). This tells us that some mass points are more difficult to classify than others, in fact such behavior is directly reflected on *single-mass interpolation* (i.e. when we train our model on just one mass less). In figure 7 we can observe how interpolating \mathcal{D}_{500} (plot d) is way more difficult than the other masses. This also suggests us that evaluating our model on only one mass less does not necessarily imply that our network will correctly interpolate everywhere, in general.

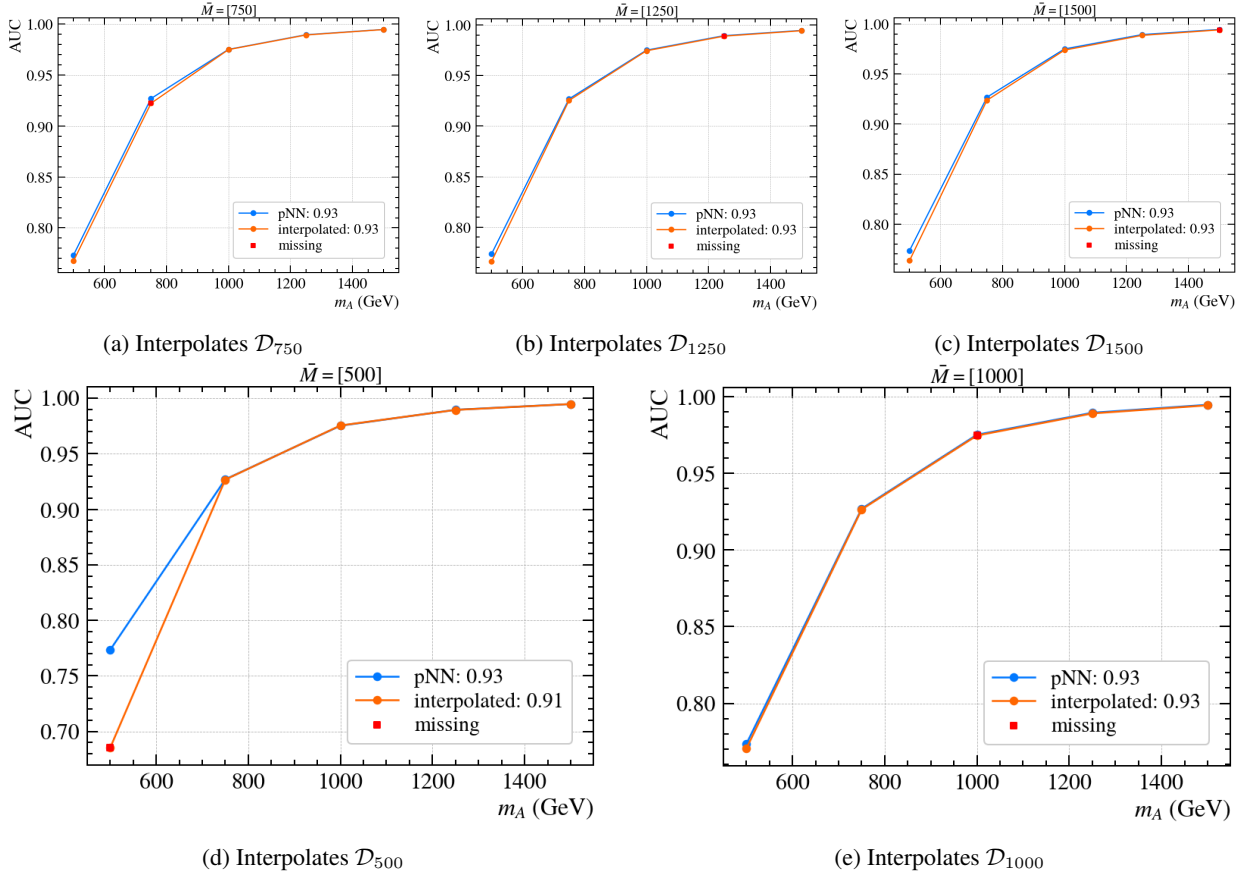


Figure 7: Single-mass interpolation on HEPMASS. The blue curve (same in all plots) represents the AUC of a pNN trained on all hypotheses. The orange curve depicts AUC performance for a pNN trained on a subset of the masses. The missing masses are denoted by a red square.

Another way to understand how much the similarity among masses helps (or avoids) our network at interpolating them, is to stress our model at *extrapolating*: i.e. we train a pNN on just *one* mass, requesting it to interpolate all the remaining ones. In figure 8 (plot a and b) we observe how easier is to interpolate the missing masses, being the model only trained on mass 750 or 1000. This fact seems to be (at least, partially) independent from the AUC achieved on such mass points: although on \mathcal{D}_{1500} the highest AUC is obtained (plot 8e), extrapolation performance are not the highest among the others.

- **Background distribution and Regularization:** the impact of background distribution (section 4.2) goes beyond classification performance, as it may also affect interpolation. Figure 12c denotes a pNN that hardly interpolates; such network was trained on a *uniformly distributed* background, without regularization. During training we noticed that such network was able to almost classify perfectly both the training and validation

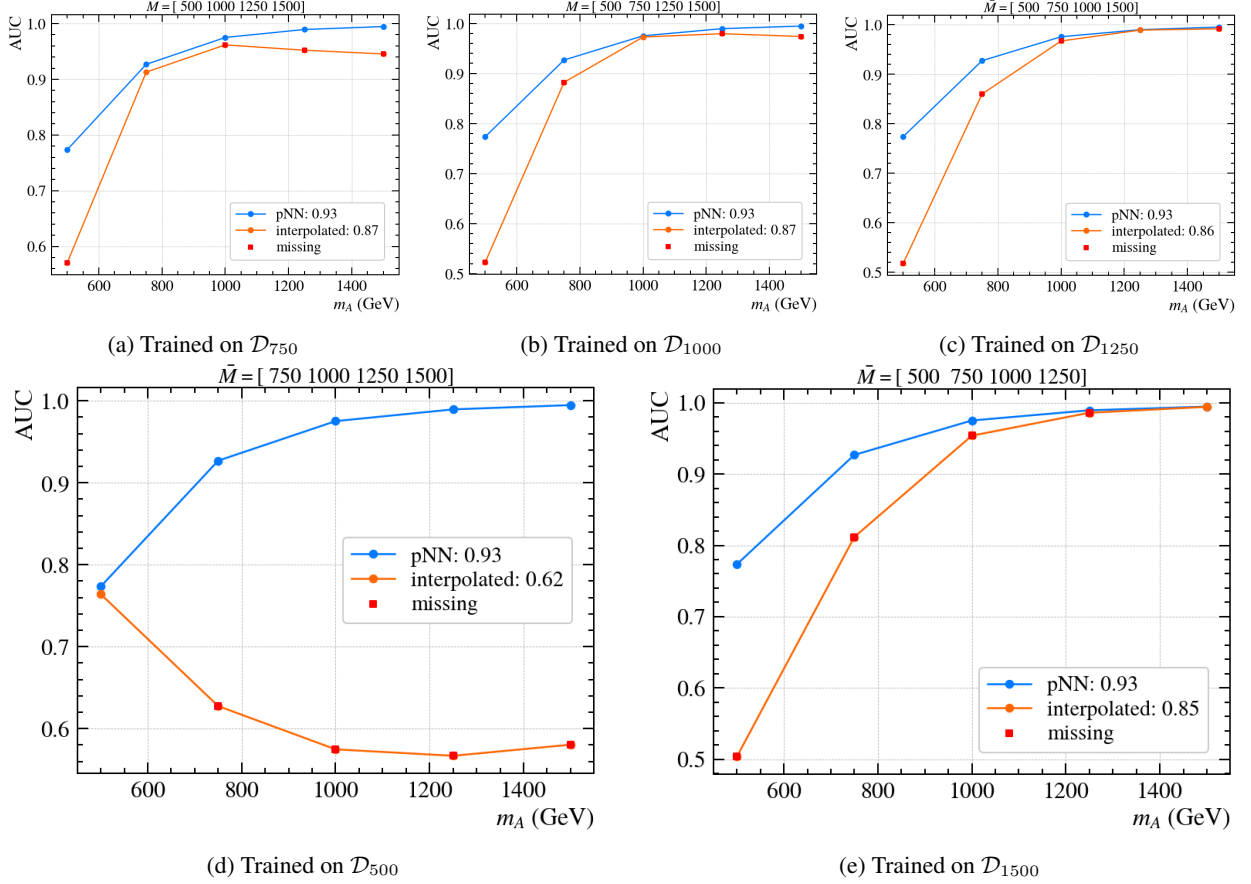


Figure 8: Extrapolation on HEPMASS. We can clearly notice how different mass 500 is from all the others, in fact its extrapolation performance is really poor: the (mean) AUC decreases by more than 30%. The other plots present a mean loss in AUC that is at most 8%.

sets. As discussed previously, having a uniform m_A for the background introduces an additional correlation with the class label, making training "easy". Indeed, by regularizing the model enough and increasing the batch size, generalization as well interpolation can be achieved with success.

Select mass hypotheses. Another practical aspect to consider is how to select the mass hypotheses to drop for a fair measure of interpolation. As described earlier, the goodness of training data can mislead us when quantifying interpolation. So, we suggest to drop almost half of the mass hypotheses, in the following way: considering we have hypotheses $[m_0, m_1, m_2, m_3, m_4, m_5]$, we may drop $[m_0, m_2, m_4]$ or $[m_1, m_3]$. Sometimes, it is interesting (also useful) to see what a parametric network can achieve when trained on *only one mass*, and evaluated for extrapolation on all the others: like done in figure 8. This may be thought as an extreme interpolation test that resembles the training of individual classifiers, being different in that also the mass feature is provided. This kind of test can be useful to better understand the contribution of both network architecture and training data, to the quality of the resulting interpolation: in this case, we can expect the parametrized network (trained on only one mass) to perform well on the only training mass, but not too worse on immediately "close" hypotheses also maintaining a reasonable accuracy on "far" masses. This can be an easy way to assess the similarity of features among masses (which is an intrinsic property of the training data): if masses are similar, the network should perform almost the same on each unseen mass.

5.2 Learned Mass Representation

Recall from section 1 that in our signal-background classification problem we actually consider \mathcal{M} mass hypotheses for the signal, this means that our original task can be broken down into \mathcal{M} smaller classification problems, each of them considering only a specific mass $m_i \in \mathcal{M}$. In fact, approaches before the parametric network [5] used to solve each sub-task by training a neural network solely on \mathcal{D}_{m_i} (i.e. a slice of the original dataset \mathcal{D} , that selects events whose

mass feature is m_i). Thus obtaining a (disjoint) set of \mathcal{M} individual networks, which we will call g_{m_i} (or g_i for short). Somehow each individual network g_i , despite being trained solely on one m_A , is able to *implicitly* relate the input features to the signal hypothesis m_i they truly belong to (or even to the underlying invariant mass). This fact seems to be confirmed by the visualization in figure 9, in which each intermediate representation h_i (of network g_{m_i} for all $m_i \in \mathcal{M}$) has a precise and nicely clustered spatial arrangement, that also relates well to the learned class label.

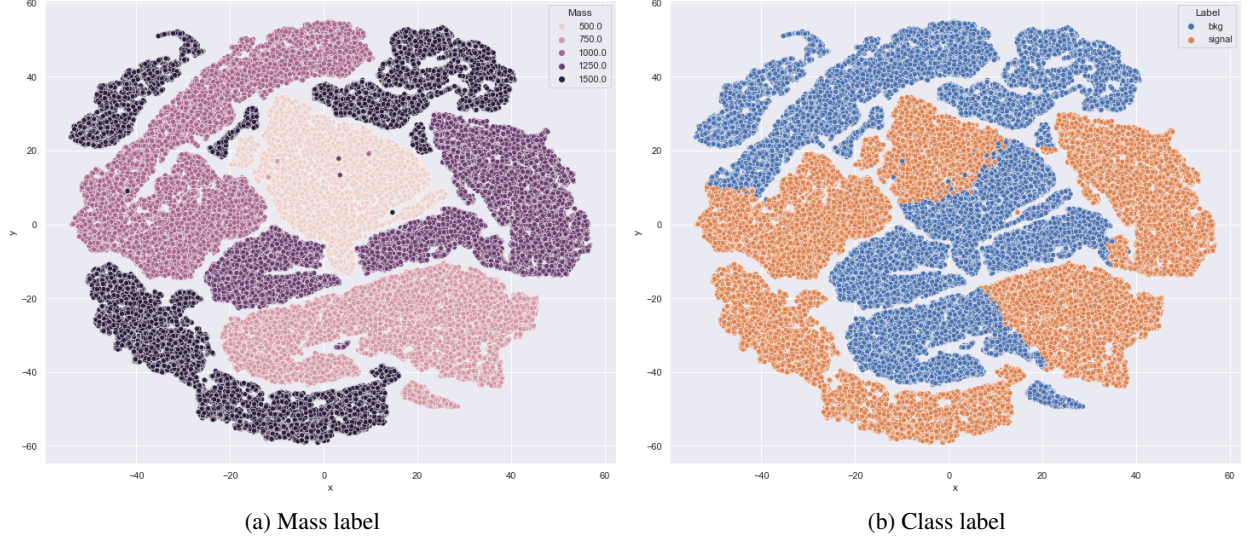


Figure 9: Visualization of the intermediate learned representation (i.e. last hidden layer) of each individual network by means of t-SNE [21, 22] on the HEPMASS dataset. By coloring the points by the mass label (left plot), we notice that representations related to the same mass are clustered together, meaning that each network g_i has indirectly acquired knowledge about its underlying mass m_i (although not given as input). Also a structured part of them clearly depicts the learned class label (right plot).

Such kind of visualizations may provide further insights about the relation existent between a parametric network and a set of individual networks. Intuitively, we may want the intermediate representation of our pNN to be disentangled along the *mass "axis"* (in the underlying manifold), as seen in figure 9 for individually trained neural networks (considered as a whole). The situation for the pNN is similarly structured (figure 10): some mass are well clustered (e.g. 500mA) and for others we can observe a smooth "shading" among them. This means that the pNN has *partially* recovered the underlying structure about the individual masses, but there is still some confusion about representing datapoints coming from higher values of the signal mass hypotheses.

6 Evaluation

Since the datasets we have for signal-background classification can be divided into $|\mathcal{M}|$ groups (in order to be able to "parametrize" a neural network), also evaluation metrics have to be considered in terms of the available mass hypotheses for the signal. In particular, the models are evaluated on each m_A separately. So we consider the signal events generated at a certain $m_i \in \mathcal{M}$, along with the whole background: i.e. the background events that spans the entire mass range. Indeed, the results provided in this section were all computed only on the test-set of the respective datasets. Moreover, we *weight* both signal and background samples (only for evaluation) such that the weighted count of signal events is equal to the weighted count of background events, i.e:

$$\sum_i w_s^{(i)} = \sum_j w_b^{(j)}$$

In particular, for both datasets we set the signal weight to one, $w_s = 1$, and for the background as $w_b = 1/5$; since we have five mass hypotheses for the signal. For such reason, each time we test a particular mass hypothesis $m_i \in \mathcal{M}$, we select the corresponding signal (i.e. all the signal events that have m_i as mass feature) and the *whole* background: i.e. the mass feature of all background samples is set to equal to m_i .

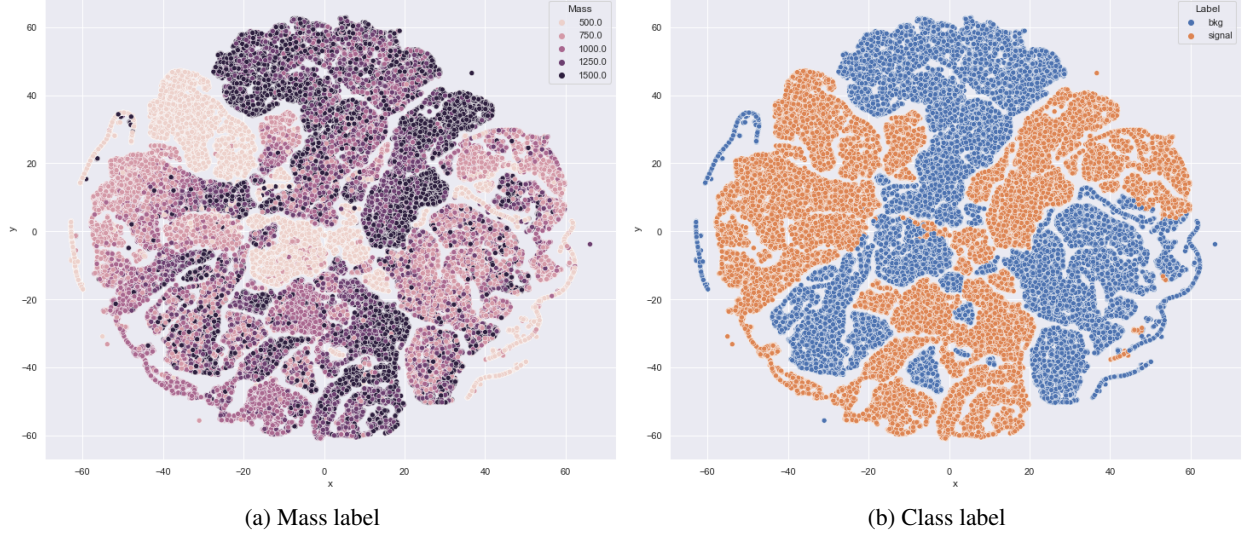


Figure 10: Visualization of the intermediate learned representation of a pNN trained on the HEPMASS dataset. Compared to figure 9, some structure is present although more convoluted, and less clear in general.

6.1 Metrics

We consider standard evaluation metrics for classification tasks, such as the *AUC* (area under the curve) of the *ROC* (receiving operating characteristic) and *Precision-Recall* curves. In particular, the ROC curve can be interpreted for HEP as comparing the *signal efficiency* (y -axis) against the *background efficiency* (x -axis): in terms of how much signal is retained when considering a certain fraction of the background. Otherwise, we can consider the *background rejection* (i.e. $1 - \text{background efficiency}$): how much signal is retained at a certain discard of background. The Precision-Recall curve instead, compares the signal efficiency (*recall*) with what we call the *purity* (precision): the number of true signal divided by the number of events classified as signal (which also contains misclassification of the background).

Along usual classification metrics, we also consider the *Approximate Median Significance* (AMS) [2] but in the following form [6]:

$$\text{AMS}(t) = \frac{s_t}{\sqrt{s_t + b_t}} \quad (1)$$

In which s_t and b_t is the (weighted) number of *true* signal and true background events, respectively, that passed the classification threshold t . This quantity is useful to determine an optimal classification threshold for our networks, called the *best cut* t^* , that is the cut that maximizes the significance: $t^* = \arg \max_t \text{AMS}(t)$. Since the value of the AMS depends on the number of events from which is calculated, we propose a new metric the *significance ratio* (σ_{ratio}) that is normalized in $[0, 1]$, thus being very intuitive to interpret. The significance ratio is defined as the ratio between the best (maximum) AMS by the largest possible significance (only achievable ideally, by means of a perfect classification when $s_t = s_{\text{max}}$, i.e. equal to all the true signal, and $b_t = 0$):

$$\sigma_{\text{ratio}} = \frac{\max_t \text{AMS}(t)}{s_{\text{max}} / \sqrt{s_{\text{max}}}} = \max_t \left\{ \frac{s_t \cdot \sqrt{s_{\text{max}}}}{s_{\text{max}} \cdot \sqrt{s_t + b_t}} \right\} = \frac{s_* \cdot \sqrt{s_{\text{max}}}}{s_{\text{max}} \cdot \sqrt{s_* + b_*}}, \quad (2)$$

where $s_* = s_{t^*}$, and $b_* = b_{t^*}$. Such metric can be also used to compare how well the same model classifies different mass hypotheses: this is now possible since the number of events belonging to a certain m_A does not affect the scale of the metric (as happens for the AMS, instead), anymore. We can further say that the best cut t^* , apart from telling us which classification threshold is the best to determine the positive class, is also an useful quantity to monitor because it can provide additional information about the goodness of the classification. In particular, by plotting the best cut versus the m_A we may observe failure cases in which t^* is either 0 or 1, depicting a situation in which the network is unable to correctly separate out the background ($t^* = 0$) or to retain a significant amount of signal ($t^* = 1$). A special failure case can be observed when $s_* = s_{\text{max}}$ and $s_* = b_*$: i.e. the signal is equal in number to all the true signal, which is also equal to the true classified background (e.g. due to applied weights). In this case we would obtain $\sigma_{\text{ratio}} = 1/\sqrt{2} \approx 0.707$, since:

$$\frac{s_* \cdot \sqrt{s_{\text{max}}}}{s_{\text{max}} \cdot \sqrt{s_* + b_*}} \xrightarrow{s_* = s_{\text{max}}} \frac{\cancel{s_*} \sqrt{s_*}}{\cancel{s_*} \sqrt{s_* + b_*}} \xrightarrow{s_* = b_*} \frac{\sqrt{s_*}}{\sqrt{s_* + s_*}} = \frac{1}{\sqrt{2}} \quad (3)$$

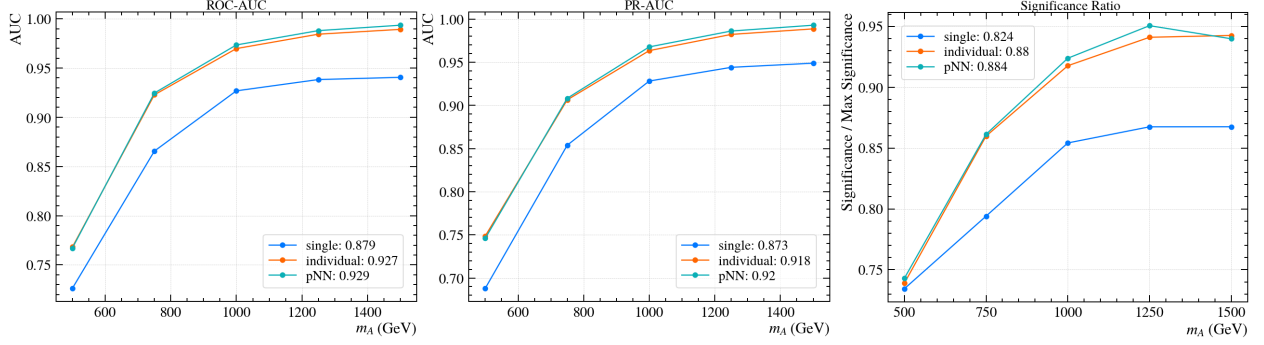


Figure 11: Comparison among (tuned) baselines on HEPMASS-IMB. As we can see, the best classification performance (in terms of ROC, PR, and σ_{ratio} for each $m_i \in \mathcal{M}$) are achieved by the individual NNs, as well as the parametric baseline (with identical-fixed m_A distribution for the background's mass feature).

Indeed, measuring $\sigma_{\text{ratio}} \approx 0.707$ also implies having an AUC of 0.5, corresponding to nonsense classification. Moreover, if the best cut t^* is such that $s_* = s_{\text{max}}$ but $b_* > 0$, then $\sigma_{\text{ratio}} = \frac{\sqrt{s_*}}{\sqrt{s_* + b_*}}$ decreases toward zero (in the limit), as b_* approaches b_{max} (i.e. the weighted count of all true background events).

6.2 Baselines

To first assess the advantages brought by parametric neural networks we should compare them to their "non-parametric" counterparts, namely *single* and *individual* neural networks. What we call a single-NN is just a neural network that is trained *without* the mass feature (m) as input but on all m_A at the same time; so, it has only one input: the features x . Instead, the individual networks are, as the name suggests, a set of single networks, g_{ϕ_i} , each of them trained to target a specific mass hypothesis $m_i \in \mathcal{M}$. Since each g_{ϕ_i} is trained in isolation on one m_A against the whole background, we expect the individual networks to easily beat the single network as it should face a harder learning problem. Moreover, both kind of networks can provide baseline performance for interpolation: the single network is trained to fit all data regardless of the mass (not given as input), whereas each individual network g_{ϕ_i} will interpolate by means of the *similarity* between the hypothesis m_i it was trained on, and the m_j to interpolate.

Finally, to assess the effectiveness of the various decision choices described in section 4, we apply them (whether possible) to the non-parametric baselines, and also (of course) to the parametric baseline: a *vanilla pNN*, as intended by Baldi et al [4]. Results for classification performance are shown in figure 11.

6.3 Results

Hyperparameters. All the neural networks used for comparison are built using the TensorFlow 2.X [1] framework along with the Keras [8] library for Python. To improve reproduce our results we fix the *random seed* to be 42. All the networks use the same hyperparameters: ReLU activation, [300, 150, 100, 50] units for each hidden layer, sigmoid output, binary-crossentropy loss, Adam optimizer [17], batch size of 1024 (except when told otherwise), and default initialization: *glorot_uniform* for weights, and constant *zero* initializer for biases; resulting in just about 70k learnable parameters. The learning rate is never decayed, and set to $3e-4$. In general, we always use regularization by means of both dropout (with drop rate of 25%), and $l2$ -weight decay. The weight decay is applied differently: with a strength of $1e-4$ for weights (or $1e-5$), and $1e-5$ for biases (or $1e-6$). Also the same hyperparameters are kept for both datasets, as well as the training budget fixed at 25 epochs.

HEPMASS. Results about classification performance (with baseline models), m_A distribution, and model architecture are presented in table 3. Whereas further results for interpolation are showed in figure 12; plot (a) and (b).

HEPMASS-IMB. A comparison among baseline models, parametric architectures, m_A distribution, and training procedure is detailed in table 5. Further results on interpolation are presented both in table 4 and figure 12c. Finally, outcomes about classification performance in terms of class separation are detailed in figure 13.

Model		Mass (GeV)					AUC (average)
Kind	m_A Distribution	500	750	1000	1250	1500	
Single-NN	None	68.55	89.37	96.38	98.07	98.69	90.21%
Individual-NNs	None	77.35	92.59	97.42	98.89	99.45	93.14%
pNN	uniform (<i>fixed</i>)	70.95	91.80	97.26	98.79	99.37	91.63%
Affine	uniform (<i>fixed</i>)	71.24	90.81	96.94	98.64	99.26	91.38%
pNN	uniform (<i>sampled</i>)	71.63	91.71	97.25	98.82	99.39	91.76%
Affine	uniform (<i>sampled</i>)	70.16	91.61	97.16	98.75	99.34	91.40%
pNN	identical (<i>fixed</i>)	76.78	92.56	97.46	98.92	99.46	93.04%
Affine	identical (<i>fixed</i>)	77.34	92.80	97.55	98.96	99.49	93.23%
pNN	identical (<i>sampled</i>)	76.77	92.60	97.48	98.92	99.46	93.05%
Affine	identical (<i>sampled</i>)	77.31	92.77	97.55	98.96	99.49	93.22%

Table 3: Per-mass ROC's AUC metric computed on the test-set of HEPMASS: all AUC values are in percentage, higher is better. Best values in boldface.

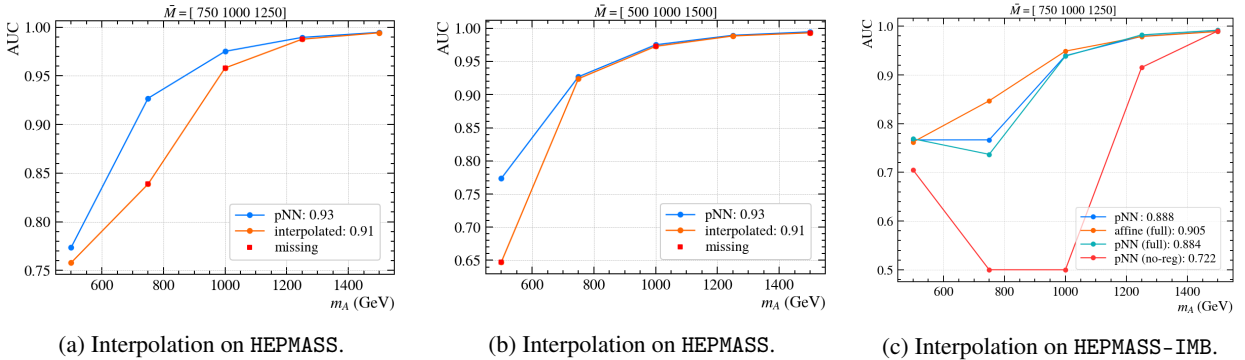


Figure 12: In figure (a) and (c) the models have been trained solely on two mass hypotheses: 500 and 1500; instead, 750 and 1250 for plot (b). In particular, in figure (c) we can see how the lack of proper regularization prevents the network (depicted by the red line) to interpolate the signal at the missing mass hypotheses.

7 Conclusions

In this study we first discussed the concept of "parametrization" (or parametric) which is really a re-brand of the widely used conditioning mechanisms in deep learning. Establishing such connection allows us to brought ideas and methods from such area, to improve pNNs in HEP. Another proposed intuition is about the structure of the data we use for signal-background classification: we know the contribution of the background(s), and at which mass the signal is generated. In fact we leverage the latter information to build a mass feature that parametrizes a neural network, allowing the model to replace a set of individual classifiers, as well as to interpolate beyond events seen during training. By studying the general structure of the data, we can exploit the inductive biases it provides by embedding them in the network design, and training as well. Lastly we demonstrated that pNNs are able to interpolate under real-world assumptions. We hope the ideas proposed here to be inspirational for further work about parametric networks, but also to be useful in other fields beyond HEP that have a similar problem setting and requirements.

Open Questions. Our work is a first step towards a full understanding of parametric networks. We believe more properties and extensions to what is presented here to exist. In particular, we may suggest further research directions: (1) real-world datasets are imbalanced, so either *self-supervised learning*, class- or mass-specific *data augmentation*, or (parametric) *generative models* may provide a major improvement in classification performance; (2) the signal is generated at few discrete mass hypotheses, what about parametrizing on the whole, *continuous* mass range? Lastly, (3)

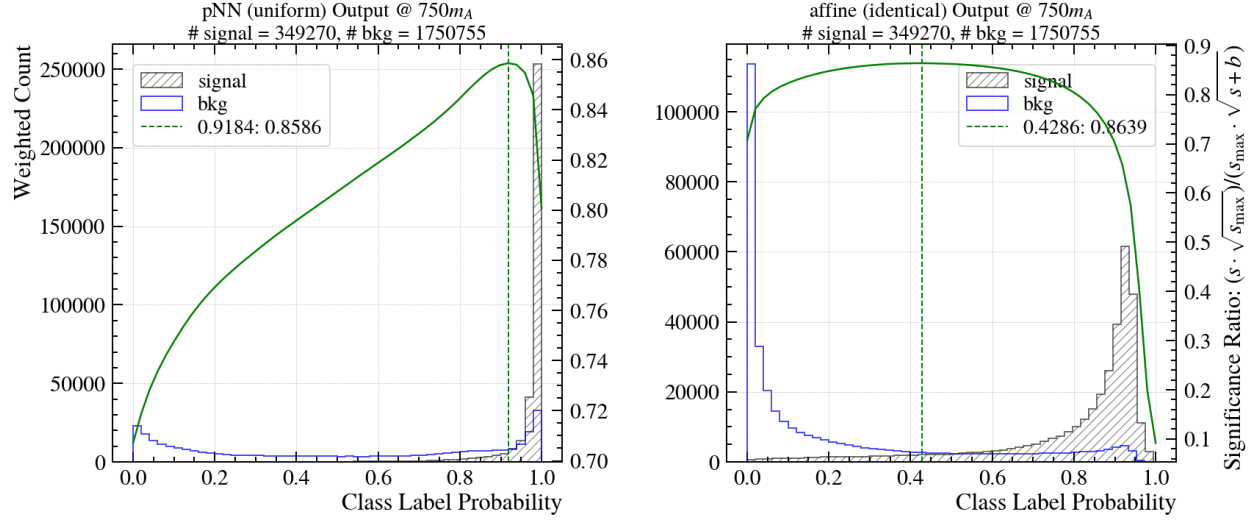
Kind	Model m_A Distribution	Mass (GeV)					Average (%)	
		500	750	1000	1250	1500	AUC	σ_{ratio}
pNN	identical (<i>sampled</i>)	76.65	76.66	93.93	97.92	98.93	88.82	
		73.77	74.08	88.06	92.37	89.14		83.48
pNN (full)	identical (<i>sampled</i>)	76.88	73.69	93.85	98.21	99.17	88.36	
		74.30	75.21	88.40	93.58	92.73		84.84
Affine (full)	identical (<i>sampled</i>)	76.20	84.68	94.87	97.87	98.89	90.50	
		73.96	80.26	89.03	92.75	89.05		85.01

Table 4: Interpolation on HEPMASS-IMB: the missing hypotheses are $\bar{\mathcal{M}} = \{750, 1000, 1250\}$. Best results in boldface.

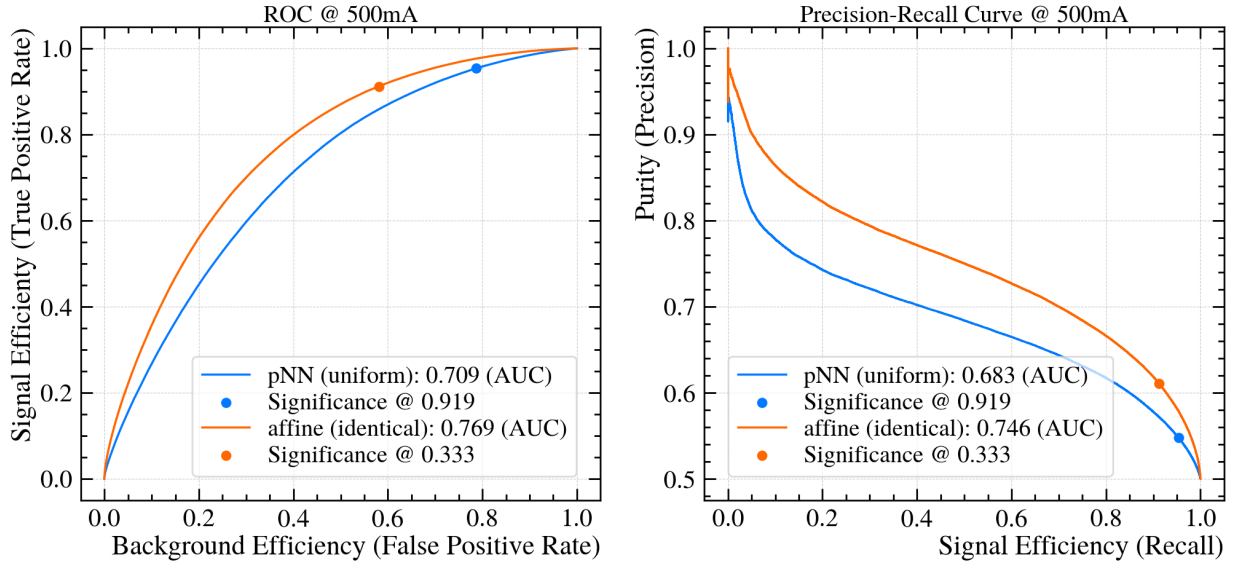
the output of a pNN is a single number, why not letting the network output or discover a *classification rule* that can be easily interpreted by physicists to further increase their knowledge about a certain phenomena?

Model		Mass (GeV)					Average (%)	
Kind	m_A Distribution	500	750	1000	1250	1500	AUC	σ_{ratio}
Single-NN	None	72.62	86.56	92.68	93.83	94.06	87.95	
		73.32	79.38	85.36	86.73	86.75		82.31
Individual-NNs	None	76.81	92.28	96.98	98.44	98.93	92.69	
		73.87	85.96	91.60	93.43	92.83		87.54
pNN	identical (<i>fixed</i>)	76.71	92.46	97.35	98.8	99.35	92.93	
		74.29	86.11	92.37	94.47	92.20		87.89
pNN (full)	identical (<i>fixed</i>)	76.29	92.33	97.33	98.79	99.34	92.82	
		74.17	86.14	92.44	95.18	96.30		88.85
Affine (full)	identical (<i>fixed</i>)	76.45	92.46	97.38	98.78	99.31	92.88	
		74.12	86.23	92.50	95.07	94.77		88.54
pNN	identical (<i>sampled</i>)	76.71	92.46	97.35	98.8	99.35	92.93	
		74.37	86.11	92.33	94.28	92.01		87.82
pNN (full)	identical (<i>sampled</i>)	76.38	92.39	97.34	98.79	99.34	92.85	
		74.14	86.16	92.46	95.16	96.42		88.87
Affine (full)	identical (<i>sampled</i>)	76.41	92.43	97.37	98.80	99.34	92.87	
		74.12	86.18	92.47	95.09	94.90		88.55
pNN	uniform (<i>fixed</i>)	76.67	92.41	97.33	98.79	99.34	92.91	
		74.28	86.09	92.36	94.73	93.03		88.10
pNN (full)	uniform (<i>fixed</i>)	72.20	91.41	97.11	98.70	99.25	91.73	
		72.17	85.42	92.16	94.93	96.23		88.18
Affine (full)	uniform (<i>fixed</i>)	67.02	91.15	97.08	98.70	99.30	90.65	
		70.71	85.39	92.04	94.88	96.34		87.87
pNN	uniform (<i>sampled</i>)	72.20	91.48	97.17	98.72	99.29	91.77	
		72.82	85.54	92.11	94.82	95.05		88.07
pNN (full)	uniform (<i>sampled</i>)	71.35	91.54	97.18	98.73	99.31	91.62	
		71.50	85.43	92.19	94.98	96.44		88.11
Affine (full)	uniform (<i>sampled</i>)	66.08	90.37	96.82	98.51	99.14	90.18	
		71.90	84.85	91.55	94.40	95.91		87.72

Table 5: Comparison of baselines, model architecture, background's m_A distribution, and training procedure on HEPMASS-IMB. Performances are evaluated in terms of ROC-AUC and AMS ratio.



(a) Weighted class separation (histograms), significance ratio (solid green curve), and best-cut (vertical dashed green line), at 750 GeV. The value of the best cut (classification threshold), and the corresponding value of the significance ratio are shown in the legend at the top-left corner.



(b) Comparison of ROC and PR curves at 750 GeV.

Figure 13: Comparison of classification performance on HEPMASS-IMB, between a pNN (uniform, fixed) and affine model (identical, fixed). We can notice how the two models opt for rather different classification thresholds.

References

- [1] M. Abadi, P. Barham, J. Chen, Z. Chen, A. Davis, J. Dean, M. Devin, S. Ghemawat, G. Irving, M. Isard, et al. Tensorflow: A system for large-scale machine learning. In *12th {USENIX} symposium on operating systems design and implementation ({OSDI} 16)*, pages 265–283, 2016.
- [2] C. Adam-Bourdarios, G. Cowan, C. Germain, I. Guyon, B. Kégl, and D. Rousseau. The higgs boson machine learning challenge. In *NIPS 2014 Workshop on High-energy Physics and Machine Learning*, pages 19–55. PMLR, 2015.
- [3] P. Baldi, K. Cranmer, T. Faucett, P. Sadowski, and D. Whiteson. Hapmass dataset - uci machine learning repository. 2015. <http://archive.ics.uci.edu/ml/datasets/HEPMAS>.
- [4] P. Baldi, K. Cranmer, T. Faucett, P. Sadowski, and D. Whiteson. Parameterized neural networks for high-energy physics. *The European Physical Journal C*, 76(5):1–7, 2016.
- [5] P. Baldi, P. Sadowski, and D. Whiteson. Searching for exotic particles in high-energy physics with deep learning. *Nature communications*, 5(1):1–9, 2014.
- [6] D. Bonacorsi, S. Marcellini, F. Primavera, T. Diotallevi, and W. Korcar. Search for beyond standard model neutral higgs boson in the $\mu\mu$ channel with the cms detector at lhc with a multivariate approach. 2019.
- [7] S. Chatrchyan, V. Khachatryan, A. M. Sirunyan, A. Tumasyan, W. Adam, E. Aguilo, T. Bergauer, M. Dragicevic, J. Erö, C. Fabjan, et al. Observation of a new boson at a mass of 125 gev with the cms experiment at the lhc. *Physics Letters B*, 716(1):30–61, 2012.
- [8] F. Chollet et al. keras, 2015.
- [9] F. Codevilla, M. Müller, A. López, V. Koltun, and A. Dosovitskiy. End-to-end driving via conditional imitation learning. In *2018 IEEE International Conference on Robotics and Automation (ICRA)*, pages 4693–4700. IEEE, 2018.
- [10] A. Collaboration et al. Search for charged higgs bosons decaying into a top quark and a bottom quark at $\sqrt{s} = 13$ tev with the atlas detector. *arXiv preprint arXiv:2102.10076*, 2021.
- [11] C. Collaboration. Search for a charged higgs boson decaying into top and bottom quarks in proton-proton collisions at 13tev in events with electrons or muons. 2019.
- [12] V. Dumoulin, E. Perez, N. Schucher, F. Strub, H. d. Vries, A. Courville, and Y. Bengio. Feature-wise transformations. *Distill*, 2018. <https://distill.pub/2018/feature-wise-transformations>.
- [13] B. Eysenbach, A. Gupta, J. Ibarz, and S. Levine. Diversity is all you need: Learning skills without a reward function. *arXiv preprint arXiv:1802.06070*, 2018.
- [14] C. Finn, P. Abbeel, and S. Levine. Model-agnostic meta-learning for fast adaptation of deep networks. In *International Conference on Machine Learning*, pages 1126–1135. PMLR, 2017.
- [15] J. Friedman, T. Hastie, R. Tibshirani, et al. *The elements of statistical learning*, volume 1. Springer series in statistics New York, 2001.
- [16] I. Goodfellow, Y. Bengio, and A. Courville. *Deep learning*. MIT press, 2016.
- [17] D. P. Kingma and J. Ba. Adam: A method for stochastic optimization. *arXiv preprint arXiv:1412.6980*, 2014.
- [18] M. Mirza and S. Osindero. Conditional generative adversarial nets. *arXiv preprint arXiv:1411.1784*, 2014.
- [19] A. M. Sirunyan, A. Tumasyan, W. Adam, F. Ambrogio, E. Asilar, T. Bergauer, J. Brandstetter, E. Brondolin, M. Dragicevic, J. Erö, M. Flechl, M. Friedl, and et al. Search for resonant and nonresonant higgs boson pair production in the $b\bar{b}\ell\nu\ell\nu$ final state in proton-proton collisions at $\sqrt{s} = 13$ tev. *Journal of High Energy Physics*, 2018(1), Jan 2018.
- [20] N. Srivastava, G. Hinton, A. Krizhevsky, I. Sutskever, and R. Salakhutdinov. Dropout: a simple way to prevent neural networks from overfitting. *The journal of machine learning research*, 15(1):1929–1958, 2014.
- [21] L. Van der Maaten and G. Hinton. Visualizing data using t-sne. *Journal of machine learning research*, 9(11), 2008.
- [22] M. Wattenberg, F. Viégas, and I. Johnson. How to use t-sne effectively. *Distill*, 1(10):e2, 2016.